

University of New Mexico

## UNM Digital Repository

---

Mechanical Engineering ETDs

Engineering ETDs

---

Fall 11-9-2020

### **Prefilling Mylar capacitor edge margins to improve capacitor reliability and size**

chase Kayser

Follow this and additional works at: [https://digitalrepository.unm.edu/me\\_etds](https://digitalrepository.unm.edu/me_etds)



Part of the [Mechanical Engineering Commons](#), and the [Other Materials Science and Engineering Commons](#)

---

#### **Recommended Citation**

Kayser, chase. "Prefilling Mylar capacitor edge margins to improve capacitor reliability and size." (2020). [https://digitalrepository.unm.edu/me\\_etds/202](https://digitalrepository.unm.edu/me_etds/202)

This Thesis is brought to you for free and open access by the Engineering ETDs at UNM Digital Repository. It has been accepted for inclusion in Mechanical Engineering ETDs by an authorized administrator of UNM Digital Repository. For more information, please contact [disc@unm.edu](mailto:disc@unm.edu).

Chase Kayser

*Candidate*

---

Mechanical Engineering

*Department*

---

This thesis is approved, and it is acceptable in quality and form for publication:

*Approved by the Thesis Committee:*

Nathan Jackson Ph.D., Assistant Professor, UNM Department of Mechanical Engineering (Chairperson)

Alex Robinson, Ph.D., Distinguished Member Technical Staff, Sandia National Laboratories

Yu-Lin Shen, Ph.D., Department Chair, UNM Department of Mechanical Engineering

**PREFILLING MYLAR CAPACITOR EDGE MARGINS TO  
IMPROVE CAPACITOR RELIABILITY AND SIZE**

by  
**CHASE KAYSER**

**BACHELOR OF MECHANICAL ENGINEERING, UNM, 2018**

THESIS

Submitted in Partial Fulfillment of the  
Requirements for the Degree of

**Master of Science  
Mechanical Engineering**

The University of New Mexico  
Albuquerque, New Mexico

**December 2020**

## ACKNOWLEDGEMENTS

I would like to thank my Sandia mentor Alex Robinson for giving me the opportunity to work on a project outside of my skillset which pushed me to learn from and adapt to challenges. Alex shared knowledge not only on this project but with my career that guided me to where I am now. I greatly appreciate all he has done for me. I would like to thank my UNM advisor Nathan Jackson for his support. Nathan was always willing to help in any way possible.

I would like to show my gratitude to Judi Lavin, Keith Ortiz, Lok-kun Tsui, Ethan Secor, and Randy Schunk for supporting me with my research and allowing me to take on a work project to fulfill my academic goals. I would also like to express my appreciation to Adam Lester and Ted Parson from Sandia for their assistance with high voltage testing.

I would like to thank my family for encouraging me to reach my goals and my friends for helping me along the way.

I would like to thank Sandia National Laboratories for funding this research. Sandia National Laboratories is a multimission laboratory managed and operated by National Technology & Engineering Solutions of Sandia LLC, a wholly owned subsidiary of Honeywell International Inc. for the U.S. Department of Energy's National Nuclear Security Administration under contract DE-NA0003525

# **Prefilling Mylar Capacitor Edge Margins to Improve Capacitor Reliability and Size**

**By**

**Chase Kayser**

**B.A., Mechanical Engineering, University of New Mexico, 2018**

**M.S., Mechanical Engineering, University of New Mexico, 2020**

## **ABSTRACT**

Typical high-voltage, wound film-foil capacitors have large edge margins filled with air to prevent breakdown between foil electrodes. This arrangement is inefficient for energy density and leaves a volume where particulates may settle in an uncontrolled atmosphere. The reliability and size of high-voltage, wound film-foil capacitors could be improved by adding a material with higher breakdown strength into the edge margins. This will not only improve reliability and size but also act as a barrier to prevent foreign object debris (FOD), volatile organic compounds (VOCs), and water from damaging the capacitor's performance. This paper will discuss the process of determining a suitable material and the process of prefilling the edge margins with a material using a reel-to-reel coating machine.

## Table of Contents

ACKNOWLEDGEMENTS .....	iii
ABSTRACT .....	iv
List of Figures .....	vi
List of Tables.....	viii
Chapter 1 .....	1
1.1 Introduction .....	1
1.2 What is a Mylar Capacitor.....	5
Chapter 2 .....	9
2.1 Review of Related Literature.....	9
Chapter 3 .....	12
3.1 Methodology Material Selection .....	12
3.2 Proof of Concept .....	14
3.3 Reel-to-Reel .....	28
Chapter 4 .....	40
4.1 Conclusion.....	41
4.2 Future Work .....	42
Works Cited .....	44
Appendix .....	45

## List of Figures

Figure 1. Current Version of Buried-Foil Mylar Capacitor with no Filled Edge Margin.....	2
Figure 2. Diagram of Extended Foil Mylar Capacitor.....	6
Figure 3. Diagram of Buried Foil Capacitor Design .....	7
Figure 4. D1 Test Structure Layout.....	14
Figure 5. Diagram of how the RK Coater Functions.....	15
Figure 6. Meyer Rod Schematic Demonstrating How Wire Gauge Affects Film Thickness .....	16
Figure 7. Compression Plate Test Setup with D1 Test Structures.....	17
Figure 8. Optical Micrograph of Early Sample Structure with Voids and Air Bubbles .....	18
Figure 9. Optical Micrograph of Optimized Sample Structure Free of Voids and Defects .....	18
Figure 10. D2 Test Structure Layout.....	19
Figure 11. D3 Design of Capacitor test Structure to Separate Probing Tabs.....	21
Figure 12. D3 Test Structure with Rounded Corners and Extended Tabs.....	22
Figure 13. Capacitor Windings After Being Pressed and Annealed.....	24
Figure 14. Capacitors with Outside Dam Being Readied for Dielectric to be Placed Inside the Dam .....	25
Figure 15. Capacitors with Inside and Outside Dam Filled with Dielectric Prepped for Vacuum Process ...	26
Figure 16. Gravure to Microgravure Comparison of Contact Angle and Web-to-Roll Distance .....	29
Figure 17. Diagram of the Microgravure Coating Process.....	30
Figure 18. Polystyrene Coating Being Applied in 25 mm Stripe Pattern at the Center of Mylar Demonstrating Clean Edges and no Smearing .....	32

Figure 19. EAA Coating Being Applied in a 5 mm Stripe Pattern on Left Edge of Mylar Demonstrating Smearing .....	32
Figure 20. Viscosity vs Pressure with Minimum Force from Pump Over Various Tube Diameters to Narrow Options for Tube Purchase .....	37
Figure 21. Viscosity vs Pressure with Maximum Force from Pump Over Various Tube Diameters to Narrow Options for Tube Purchase .....	37
Figure 22. Volumetric Flow Rate vs Pressure to Determine Best Flow Rate for Variety of Viscosities .....	38
Figure 23. Viscosity vs Pressure with Potential Materials and Flow Rates.....	39
Figure 24. RK Meyer Rod Coater Used in Initial Experiments.....	45
Figure 25. Aluminum block with Foam Used After Determining Film Thickness was Independent of Speed and Pressure .....	45



## List of Tables

Table 1. List of Usable Dielectric Materials to Make Capacitors; Highlighted is the Dielectric Strength which gave a High and Low for Testing Purposes .....	13
Table 2. D2 Test Structure Results .....	20
Table 3. D3 Test Structure Testing Results .....	23
Table 4. Results from withstand voltage screening .....	27
Table 5. EAA Dilution Measurements .....	31
Table 6. List of Material Properties Used for Vitralit-UD 5134 Calculations.....	35
Table 7. Material Viscosity for Various Materials Considered in Figure 4.....	40
Table 8. Table of Maximum Flow Rates and Machine Speed for Range of Viscosities .....	40

## **Chapter 1**

### 1.1 Introduction

There exists a growing need for passive electrical components used in everything from personal electronic devices to aircraft. In particular, the aerospace industry has a growing need for smaller high-voltage capacitors.

High-voltage, wound film-foil capacitors have large edge margins filled with air to prevent breakdown between foil electrodes. The reliability and size of high-voltage, wound film-foil capacitors could be improved by adding a material with higher breakdown strength into the edge margins. This will not only improve reliability and size but also act as a barrier to prevent foreign object debris (FOD), volatile organic compounds (VOCs), and water from damaging the capacitor.

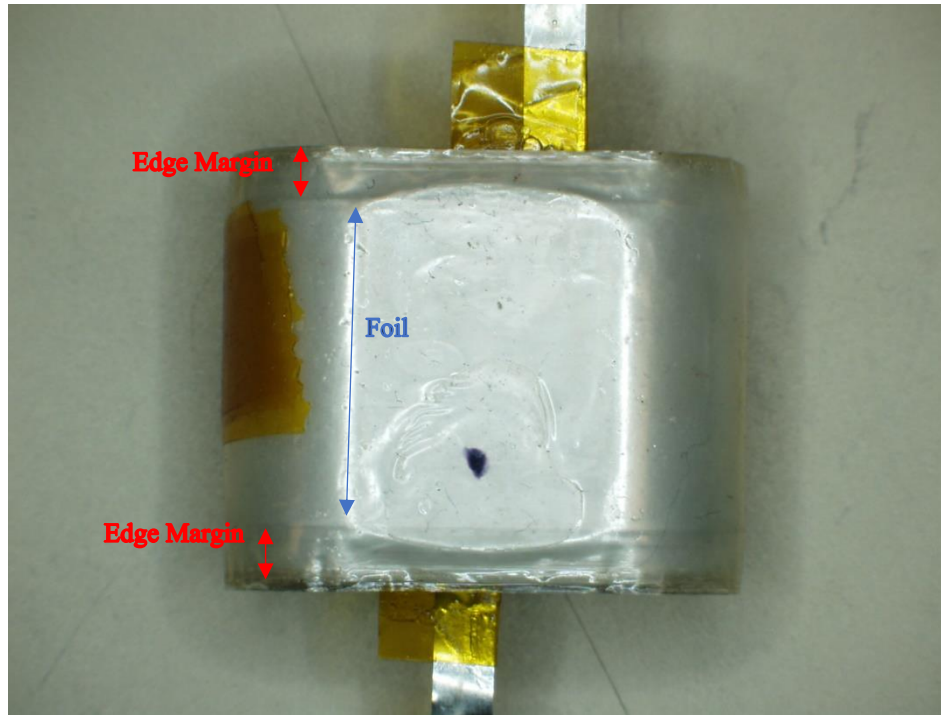


Figure 1. Current Version of Buried-Foil Mylar Capacitor with no Filled Edge Margin

Capacitors are passive devices used to store energy. In its simplest form, a capacitor is two conductive plates separated by an insulating dielectric material. When a voltage difference is applied across these plates, energy is stored in an electric field, which can be discharged quickly on demand. Capacitance relates the amount of charge stored in the capacitor to the applied voltage. This is measured as coulombs per volt with a unit known as a farad ( $F$ ). As shown in Equation 1, charge in a capacitor is proportional to both the capacitance and the applied voltage, where  $C$  is the capacitance,  $q$  is the amount charge, and  $V$  is the applied voltage.

$$q = CV \tag{1}$$

Equation 2 shows that stored energy ( $E$ ) is proportional to capacitance and the square of the applied voltage.

$$E = \frac{1}{2}CV^2 \quad (2)$$

To get more charge or energy, either increase the voltage or the capacitance. Equation 3 shows increasing capacitance can be accomplished by adding a material with a higher dielectric value between the two plates of the capacitor, increasing the area of the plates, or decreasing the separation between them. In Equation 3,  $C$  is the capacitance,  $\epsilon_r$  is the dielectric constant,  $\epsilon_0$  is the dielectric constant of a perfect vacuum,  $A$  is the area of the plates, and  $d$  is the distance separating the plates.

$$C = \epsilon_r \epsilon_0 \frac{A}{d} \quad (3)$$

For example, adding a material between the plates such as PTFE (Teflon), with a dielectric constant of 2.1, and holding everything else constant, the capacitance will double when compared to an air-filled capacitor. This also applies to rolled capacitors, which are essentially parallel plate capacitors rolled into a spiral. Rolled capacitors are treated as double-sided plate capacitors because the spiral shape creates capacitive energy storage on both sides of each electrode plate (except for the first and last full revolution). The dielectric material increases the capacitance while providing mechanical stability to the device with the plates held in very close proximity.

As can be determined from Equation 3, if the voltage is increased, the energy will increase exponentially. However, every material has a limited working voltage range determined by the breakdown voltage. When more voltage is applied the chance for breakdown of the dielectric material increases. It is important to understand a dielectric material's safe working voltage stress, or voltage rating, which is often rated in volts per milli-inch (mil) or per millimeter. This rating will help determine the thickness needed between electrodes for a given operating voltage. Once voltage, material thickness, and dielectric constant are known, the capacitance value is determined by the square area, or active width times the length of the spiral winding.

Certain applications for capacitors rely on their ability to quickly discharge the stored energy. For very rapid discharges with high voltage and high current density, the most common and easy-to-fabricate capacitor consists of dielectric plastic film layers co-wound with aluminum foil electrodes. These are known as wound-foil-film capacitors. An offset gap between the foil edges creates the edge margin separation of the two foils. The focus from here on will be on this type of capacitor fabricated with the robust, dielectric film polyethylene terephthalate (PET). One brand of this material is Mylar®, from DuPont Teijin Films. Because capacitors for the work in this report were fabricated from this brand of PET, they will be referred to hereafter as Mylar capacitors.

## 1.2 What is a Mylar Capacitor

Capacitor-grade Mylar is a biaxially-oriented polyethylene terephthalate (PET) film, which was developed by DuPont in the early 1950's (Wooley). It is used in many capacitor applications for its high tensile strength, chemical stability, and dielectric strength (Sorbent Systems). It has some advantages over other dielectric plastics such as its low permeability. With the standard-wound capacitor, the second dielectric material present is air, which has a moderate theoretical dielectric strength of ~3kV per millimeter. It fills the edge margins, or space separating the opposing electrodes. The minimum size of the edge margin gap is determined by the voltage that will be applied to the capacitor, the dielectric strength of the air in the gap, and a safety margin. The third material is the thin foil of the electrodes. These are commonly very thin aluminum (5-7 microns), but other conductive metals can be used. These three materials form the foundation of the Mylar capacitor. Additional parts are typically added, such as electrode leads, protective tape wrap or case, and potting.

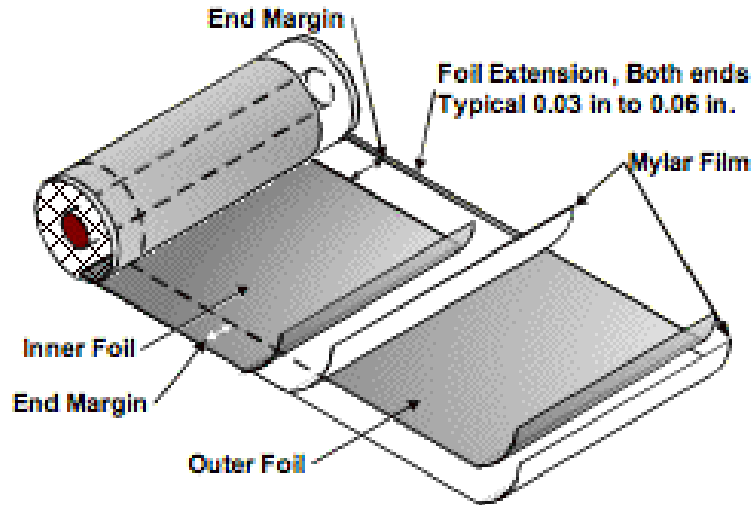
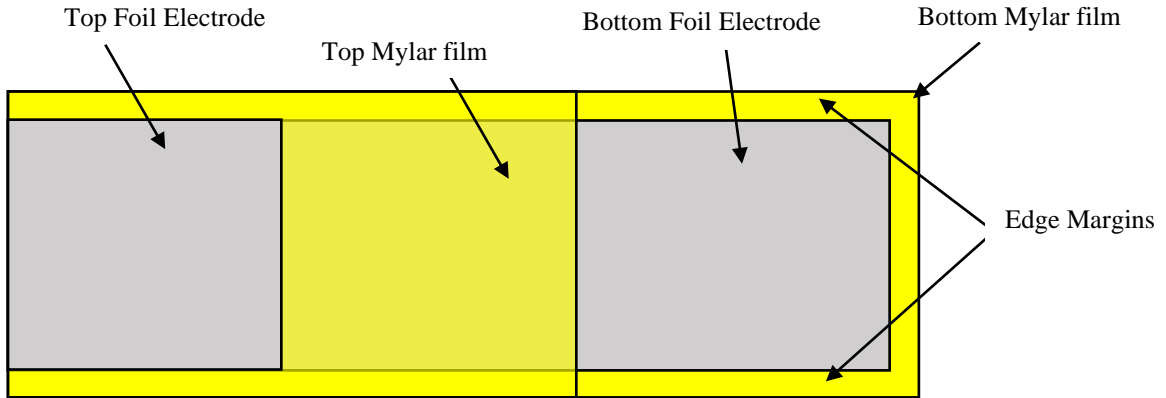


Figure 2. Diagram of Extended Foil Mylar Capacitor

Figure 2 shows an extended foil capacitor design. With this design, the first foil is laid on top of the Mylar base layer so that one edge overhangs the edge of the Mylar by  $700\ \mu\text{m}$  to  $1.5\ \text{mm}$ . The width of the foil is selected to leave a gap on the opposite side where the foil does not extend out to the edge of the Mylar. This gap is the first edge margin (a.k.a. end margin or clear margin). The next layer of Mylar is then placed on top, aligned with the base layer of Mylar. The second layer of foil is placed on top, overhanging the opposite side of the previous foil layer while creating a second edge margin. The edge margin insulates the foil electrodes from one another. Multiple layers of Mylar with various thicknesses may be used, depending on the design voltage of the capacitor.

Another construction option is the buried foil design. The layout is similar to the extended foil design except narrower foils are selected and placed in the center of the Mylar

width, leaving edge margins on both sides of each foil. This design requires tab electrodes to be inserted during the winding process.



*Figure 3. Diagram of Buried Foil Capacitor Design*

In either design, once the components are aligned, they are rolled together around a mandrel or core using a reel-to-reel machine or a winding machine. These machines can wind multiple materials from different rolls into a single capacitor winding. Foil layers start and stop at different locations to ensure electrical separation. Mylar layers make extra revolutions at the start and end to protect the active area. The outer layers are taped in place to keep the capacitor from unwinding. With extended foil designs, the overhanging foil extensions are folded over towards the center of the capacitor on both ends, creating a flat surface for electrical leads to be added.

Finishing steps vary depending on the desired casing. PET finishing tape forms a robust dielectric barrier. The exposed electrodes are then covered with an electrically insulating barrier material, such as epoxy potting. The capacitor can also be epoxy potted in a plastic housing. A more complex option involves integrating the winding into a metal



housing and impregnating it with a dielectric liquid, such as Fluorinert, gel, or oil. The liquid prevents arcing to the case and between electrodes. With proper fabrication, edge margins can be significantly reduced in size.

Despite the advantages of liquid-impregnated capacitors, there are also shortcomings. Fabrication can be costly when considering the numerous steps, production difficulty, and the casing being prone to leaking. To counteract the downfalls of liquid-impregnated designs, the concept of filling the edge margins with a dielectric barrier during the winding process has gained validity. Prefilling the edge margin could reduce the size of the edge margins, thereby decreasing overall size for a given capacitor and reducing the weight. If the same size is desirable, an increase in stored energy could be realized using this method. Filled edge margins would also prevent FOD and exchange of vapors where the electric field strength is high. These benefits can open design space while simplifying the fabrication process.

## Chapter 2

### 2.1 Review of Related Literature

Brooks identifies several configurations for a high voltage biaxially oriented PET capacitors. (Brooks) Several configurations warrant discussion, namely dry-wrap-and-fill, buried-foil Mylar, Fluorinert-filled, and extended foil Mylar capacitors. In Brooks' analysis, the Fluorinert-filled capacitors are too expensive, complex, impractical and the standard dry-wrap-and-fill and buried foil designs have too high of internal inductance. Due to increasing size constraints a new or modified capacitor design was needed. Brooks focused his research on the buried-foil design and ruled out the extended foil design due to excessively large edge margins. He did note the extended-foil design was preferred but was ultimately ruled out because of the voltage and capacitance requirements would make for excessively large edge margins. If there were a method to decrease the edge margin by applying a dielectric, the extended-foil design would have been a prime candidate with the lowest volume and inductance. (Brooks)

Herzberger and Tanner discussed extended-foil and buried-foil capacitors, specifically the dry-wrap-and-fill designs, which consist of air/Mylar windings. (Herzberger) After the capacitor is wrapped, the ends are covered with a potting material or epoxy. These two designs were put through short-term breakdown (STB) and destructive

physical analysis (DPA) to determine if arc-over failure occurred due to edge margin size or dielectric punch through from dielectric breakdown of the Mylar. Of the 40 capacitors tested, 31 failed due to arc-over with the remaining nine failing from dielectric punch through. The two types of capacitors had edge margins of 0.28 inch (7 mm) and 0.218 inch (5.537 mm). The researchers found that the failure modes which led to arc-over and dielectric punch through were curvature, insufficient inner inactive wraps, inadequate edge margins, topographical irregularities, among other less prevalent modes. (Herzberger) The most important aspect to address is the edge margin size. If there were a way to minimize the size of the edge margin while reducing the arc-over mode of failure, dimensions could be significantly reduced. The issues related to insufficient inactive wraps and topographical irregularities could be solved during the winding process by increasing the number of inactive wraps before starting the electrodes and ensuring proper tension and alignment. Adding more inner wraps would not necessarily increase the overall diameter of the capacitor if the edge margins were reduced and the effective capacitive area maintained. The overall size of the capacitor may be reduced while maintaining the desired energy density by minimizing wrinkles, entrapped air, and wandering material.

Another approach to high-voltage capacitors is an oil-free hollow cylindrical capacitor and flat format pulse capacitor. To produce these types of capacitors a special piece of equipment is required to combine the Mylar and foil. The wound capacitors are then impregnated with a thermoset low viscosity resin, which is degassed and protected from ultraviolet (UV) light. Using this technology, Sharma created extended foil capacitors rated for 10 kV and 5  $\mu$ F with a low inductance of 21 nH. (Sharma) With the oil free and

low inductance design, these capacitors function better than dry-wrap-and-fill designs. What elevates this design are the metal oil can and oil required in previous configurations. This design has great potential, however, the special machinery required to produce the impregnated capacitors is costly.

By prefilling the edge margin with a robust dielectric, relative to air, during the winding process, the failure mode of arc-over could be reduced or even eliminated. As Sharma details, the impregnated capacitor shows increased performance and reduction in size, but production is complicated by requiring special machinery to impregnate the capacitor layers during the winding process.

Brooks, Sharma, Herzberger, and Tanner preferred the extended foil design but clearly identified the large edge margins as a limitation. With the increased performance demonstrated by Sharma, a modified method to fill the edge margin during the winding process could reduce the size of the capacitor or enable increased capacitance.

## Chapter 3

### 3.1 Methodology Material Selection

The first step of producing a filled edge margin capacitor is determining what materials would meet the requirements of customer applications. For filled and sealed edge margins, the first requirement is that the material bond to the capacitor's dielectric film. The material must not deteriorate within the operational lifetime of the capacitor, often 20 years or longer. For some applications, the capacitor has a functional temperature range of  $-55^{\circ}\text{C}$  to  $+125^{\circ}\text{C}$  ( $-67$  to  $257^{\circ}\text{F}$ ) and withstand capacitor curing temperatures, which can be as high as  $150^{\circ}\text{C}$  ( $302^{\circ}\text{F}$ ). For precision deposition by a Microgravure coater, materials require a viscosity of less than 200 cP. Since the material is later wound tightly around a core or mandrel to make the capacitor, bending stress's will be generated in the material as it is wound, meaning that the material be flexible and not rigid in its final state. Another important consideration is reasonable cost of materials and processing. With the requirements outlined, a list of 20 materials was formed, listing key characteristics such as dielectric strength, dielectric constant, melting point, energy density, etc. Mylar was chosen as the film material for its dielectric properties and readily available information for coating and sealing. Polystyrene and Polyester resin in xylenes were selected from the list as filler test materials to be used in the edge margins. The cost of these materials was significantly

lower and more widely available when compared to other competitive materials. The dielectric strength of each material was significantly different which added a high and low point for testing purposes.

*Table 1. List of Usable Dielectric Materials to Make Capacitors; Highlighted is the Dielectric Strength which gave a High and Low for Testing Purposes*

<b>Film</b>	<b>Dielectric Constant</b>	<b>Dissipation Factor</b>	<b>Melting Pt., °C</b>	<b>Dielectric Strength, V/Mil</b>	<b>Volume Resistivity, Log <math>\Omega</math>-cm</b>
<i>Mylar The Gund Company (900 microns)</i>	3.20	0.20%	251	19000	17.0
<i>Polypropylene</i>	2.30	0.18%	164	5500	16.3
<i>Polysulphone_Solvay-Udel GF 110 (60Hz)</i>	3.18	0.01%	343-399	19000	16.5
<i>Polyester</i>	3.20	0.50%	254	7000	19.0
<i>Polystyrene</i>	2.56	0.00%	240	800	16.0
<i>Polycarbonate</i>	2.90	0.01%	168	2640	16.0
<i>Kapton (polyimide)</i>	3.40	0.20%	None	7700	17.2
<i>Teflon (PolyTetraFluoroEthylene)_WS Hamphsire</i>	2.10	0.01%	335	7250	18.0
<i>IMDEX (Thermoplastic Polyimide)</i>	2.50	0.14%	230	6290	17.4
<i>PVDF CS Hyde Company</i>	7.5 to 9	.01-.03		1900	
<i>ECTFE (ethylene-chlorotrifluoroethylene)</i>	2.50	0.26%	340	3200	
<i>PES (polyethersulfone)_RTP Company</i>	3.5	0.56%	343	15000	12
<i>TPX (polymethylpentene)</i>	2.12	0.00%	240	3710	16.0
<i>UHMW_Bodecker</i>	2.3	0.05%	136	2300	15
<i>PEEK (polyetheretherketone)</i>	3.30	0.26%	340	7480	16.7
<i>ULTEM (polyetherimide)</i>	3.15	0.13%	220	3050	7.8
<i>_Chemcours</i>	2.6	0.07%	260	4000	17

Both materials were thermally curable and significantly met the requirements outlined above. The two inks were commercially available and purchased from UTDOTs

Inc. The foil was 14-gauge aluminum with a width of 1 inch. It came in a roll of several hundred feet.

### 3.2 Proof of Concept

To demonstrate that the materials would function as expected, an experiment was conducted. The experiment was to 1) produce simulated edge margin structures using Mylar, Foil, and dielectric material in between foil pieces, as seen in Figure 4, and 2) test the structures by applying high voltage to characterize breakdown across the filled gaps.

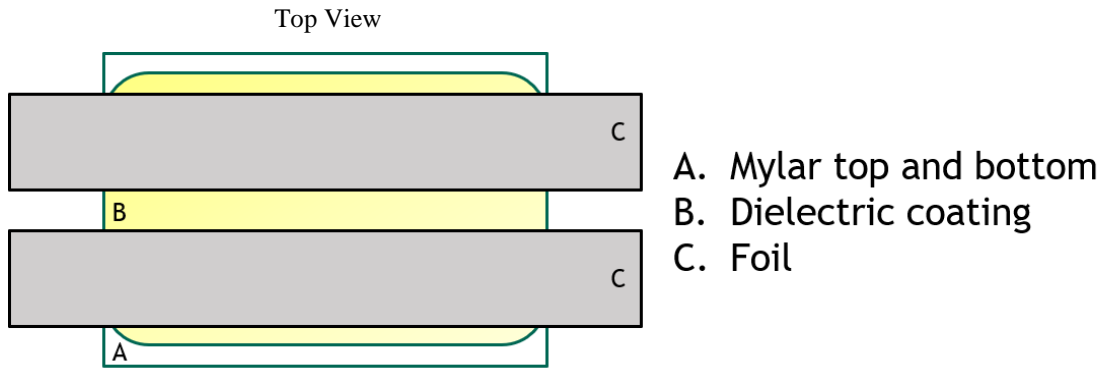


*Figure 4. D1 Test Structure Layout*

D1 Samples were constructed using 40-gauge Mylar with a thickness of 10  $\mu\text{m}$ , 24-gauge aluminum foil with a thickness of 6  $\mu\text{m}$ , and two different dielectric materials. The solutions of dielectric material were applied with an RK Meyer rod coater. The RK coater applies an even solution of the desired thickness depending on the rod used. After evaporation of the solvent, the polymer loading remains on the dielectric film.

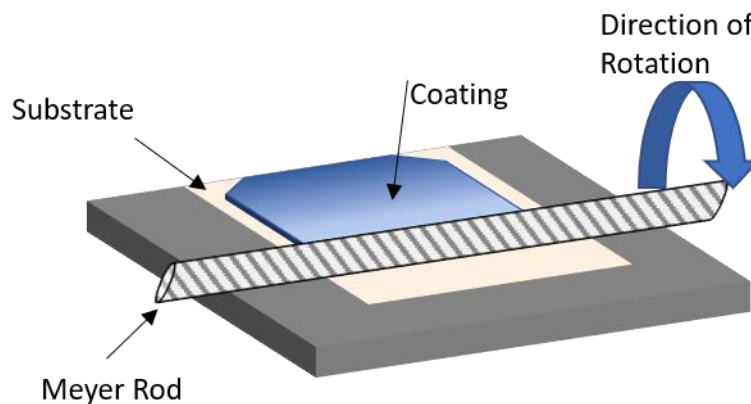


*Figure 5. Diagram of how the RK Coater Functions*

The rods vary in rating from 0-8, depending on the gauge of wire wound on the metal rod. The thickness of coating then varies depending on the rod rating. Thicker wire gauges have larger cavities filled with solution, thus resulting in a thicker deposit. Other factors do contribute to the deposition such as surface energy of the substrate, and viscosity of the coating material but typically materials with low solids loading and low viscosity (<1000 cP) tend to coat in the same manner. Surface energy of Mylar is low causing non-polar solvents like xylenes to have a hydrophilic response when applied. Being that the inks used were xylenes based it was assumed that surface energy was a negligible factor. The RK coater is an automated machine which drags the Meyer rod across the substrate, spreading the coating solution evenly. The RK coater allows the user to alter the pressure and speed at which the rod is moved across the substrate. While using the RK coater it was observed that the coating thickness was independent of speed and pressure and relied only on the gauge of wire on the rod for this application.



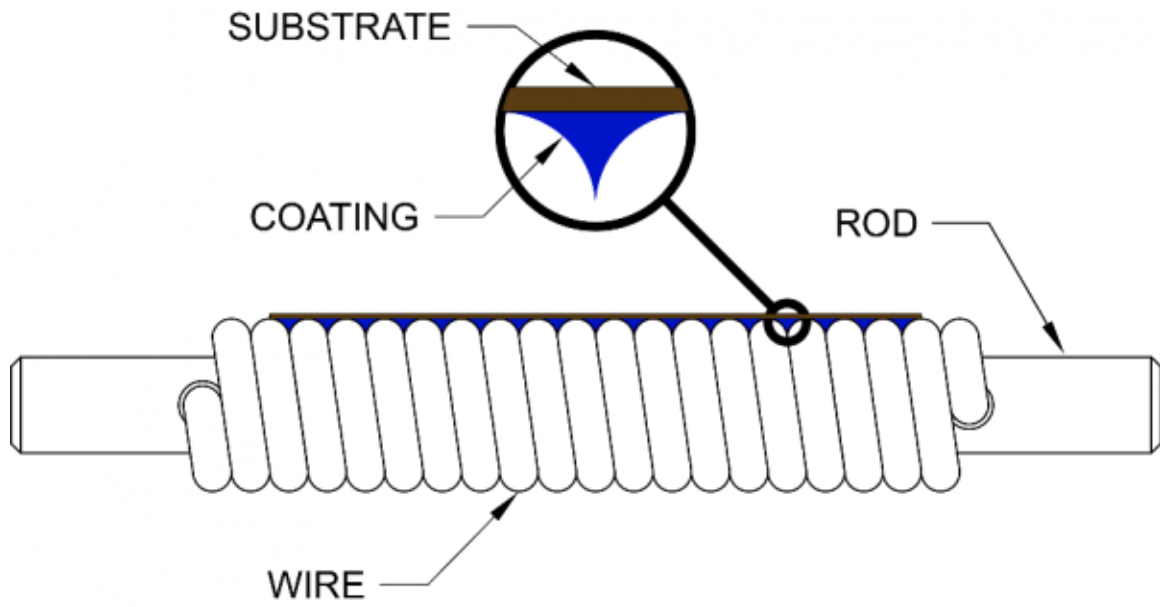


Figure 6. Meyer Rod Schematic Demonstrating How Wire Gauge Affects Film Thickness

Concluding that the coating thickness was unaffected by speed or pressure resulted in the simplification of the coating process by replacing the machine with an aluminum block covered in craft foam. The foam was in place to protect the substrate from being damaged by the block as the rod was moved across its surface. These simple test samples demonstrated that the materials used, and process applied could be successful. Still, better coating methods were needed. The Meyer rod coating was applied evenly and filled the gap between electrodes as planned, however, when a top layer of Mylar was applied the solvents in the ink would become trapped and the material would not fully dry. This allowed for air and solvent bubbles to form in the dielectric material and resulted in points of electrical breakdown failure. To avoid those defects, another approach needed to be explored.

The new approach to fabricating test structures used a vacuum oven and custom-made compression plates to laminate the thin materials together with an even layer of adhesive. The dielectric materials were applied in the gap between foil pieces using a disposable pipette. The amount of ink applied varied but a uniform coating inside the gap was achieved as excess ink would be pushed out of the gap towards the test leads. This configuration utilized a Cascade TVO5 vacuum oven and two aluminum plates secured together using nuts, bolts, and die springs for even compressive force.



*Figure 7. Compression Plate Test Setup with D1 Test Structures*

The D1 test samples maintained the same layout as with the Meyer rod approach, except the ink was applied with a pipette rather than the Meyer rod. Using a pipette ensured a precise amount of dielectric was applied. The base plate was set on a table, and a small piece of Mylar, approximately 4 inches long, was placed on top. The two foil electrodes were placed on top of the Mylar and spaced 1 mm to 5 mm using a caliper. The 2 mL of

dielectric material was applied in between electrodes using a pipette. The top layer of Mylar was placed gently on top, aligning with the bottom layer of Mylar. The top aluminum plate was placed on top to hold the completed sample together. The bolts were added from underneath, and even compression was obtained using the springs with spring constant  $k = 110 \text{ lb./in.}$  The springs were compressed 0.5 inches resulting in a force of 55 lbs. being applied to the plates. Once compression was applied, the fixtures were moved into the vacuum oven for two hours, with the temperature set to  $130^\circ\text{C}$  and vacuum to  $-83.5 \text{ kPa-g.}$  Temperature, time, and vacuum were varied to determine the best curing conditions, which was determined to be  $130^\circ\text{C}$ , for 2 hours, at  $-83.5 \text{ kPa-g.}$  These conditions produced an even and void free coating of dielectric in the gap between the foils.

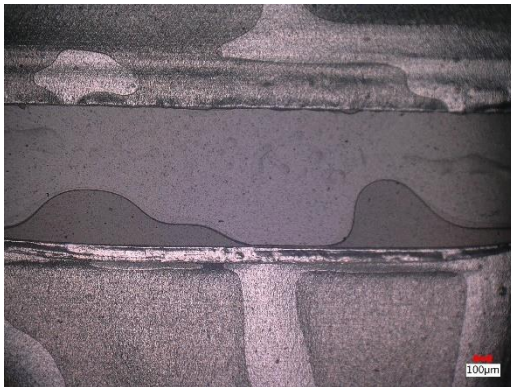


*Figure 8. Optical Micrograph of Early Sample Structure with Voids and Air Bubbles*

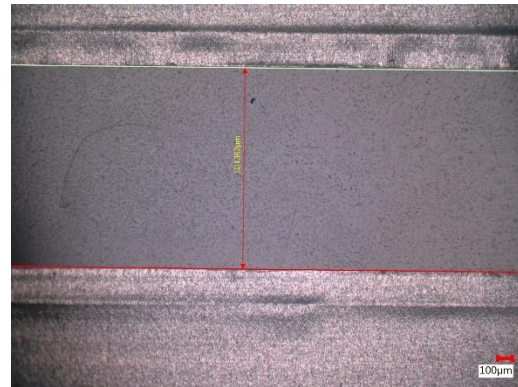


*Figure 9. Optical Micrograph of Optimized Sample Structure Free of Voids and Defects*

A revision to the design of the test structures was made to ensure no arcing occurred between the corners of the electrodes and to minimize electrical field enhancement. Field

enhancement, which occurs at sharp corners, can increase the magnitude of the electric field and cause negative effects such as corona or electrolytic breakdown. (Deken)

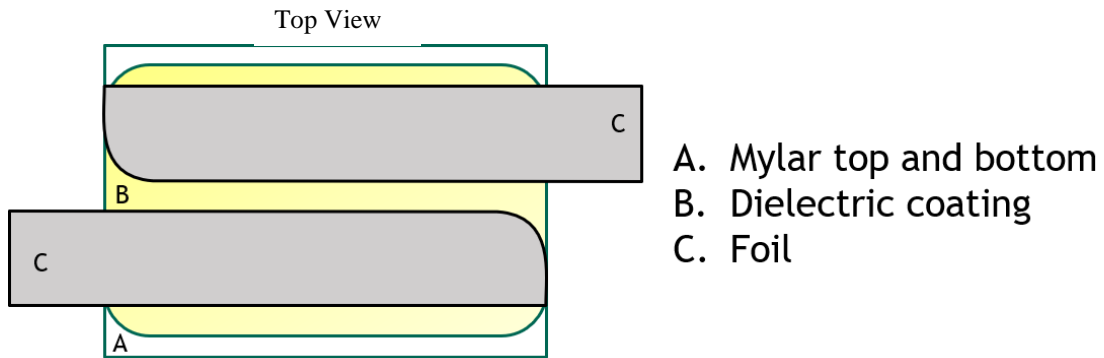


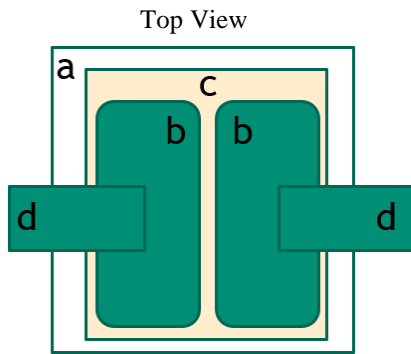
*Figure 10. D2 Test Structure Layout*

The D2 samples made with the compression plate approach underwent dielectric breakdown testing to verify the function of the dielectric material. The short-time breakdown (STB) test consisted of ramping the voltage at 250 V/s up to 20 kV at ambient temperature using a HypotMAX model 7720 DC Withstand Voltage Tester (Associated Research). Data is summarized in Table 2.

Table 2. D2 Test Structure Results

Sample Gap/ID	STB (kV)	Dielectric fill	Notes of failure
2 mm-95	18.55	Polystyrene	OG (outside gap)
3 mm-92	20.00	Polystyrene	survivor
2 mm-94 retest	11.88	Polystyrene	OG (outside gap)
3 mm	16.87	Polystyrene	OC (arced outside coating)
4 mm	20.00	Polystyrene	survivor
4 mm	20.00	Polystyrene	survivor
5 mm - 89	17.87	Polystyrene	likely OG (outside gap)
5 mm -88	20.00	Polystyrene	survivor

The data collected confirmed that gap spacings of 4 and 5 mm could survive 20 kV. 1 of the 2 samples with a 3 mm gap spacing survived 20 kV, demonstrating that a further reduction in edge-margin size could be possible. Some issues were noted with the structure design and connections of the testing instrument which required a redesign of the test samples. The redesign rounded all 4 corners of the electrode and fully encased them in the Mylar and dielectric coating. The new design decreased the size of the test sample to a 1-inch square and had the probe attachments extend out on opposite sides to limit likelihood of arcing between attachment points. All four corners were rounded this time to decrease the concentration of the electric field. The new design—referred to as D3 test structures—was based off the concept in Figure 11.



- a. Mylar sheets (top and bottom)
- b. Electrode foils
- c. Polymer dispensed in gap and around perimeter of foils
- d. Tabs – made from electrode foil laid upon the electrodes.

*Figure 11. D3 Design of Capacitor test Structure to Separate Probing Tabs*

To fabricate the rounded corners and extended tabs, a simple stamp was designed in SolidWorks, converted to an STL file, and printed on the FormLabs SLA printer. The stamp was used to hold the foil in place and act as a guide while cutting the foil with a razor blade. The test samples were formed in the same manner as before, with the aluminum compression plates, and cured in the vacuum oven using the same parameters; 130°C, 2 hours, -83.5 kPa.

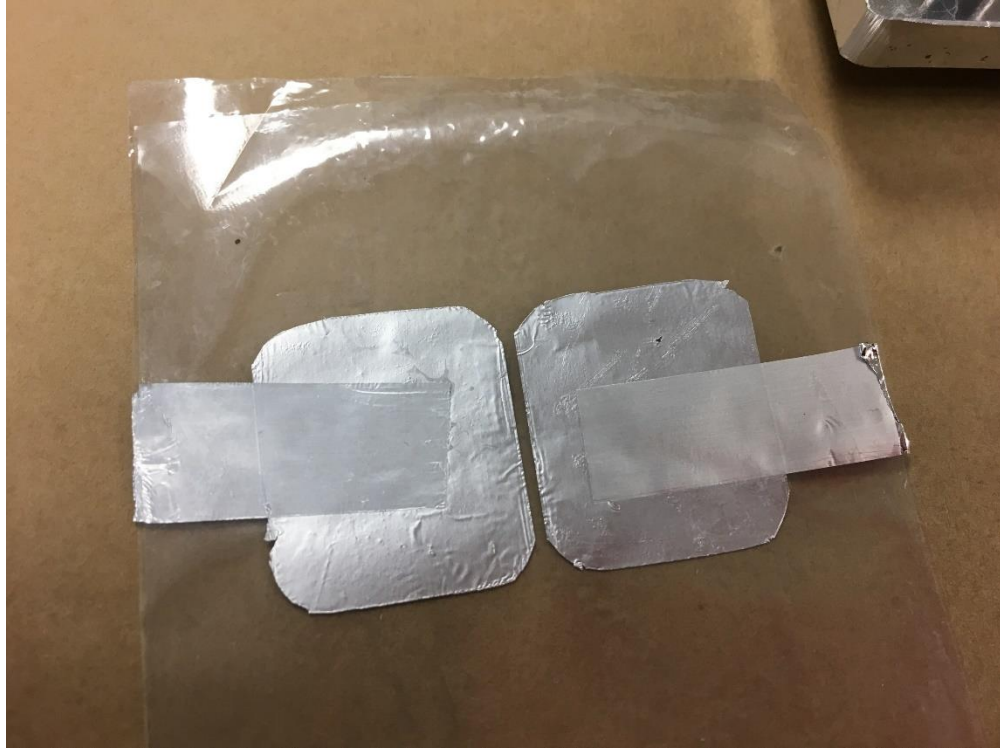


*Figure 12. D3 Test Structure with Rounded Corners and Extended Tabs*

The D3 test structures constructed with polystyrene and polyester verify the concept of filling the edge margin as a viable new approach to preventing edge margin breakdown in Mylar capacitors. Table 3 demonstrates that properly filled electrode gaps as small as 1.2 mm could withstand 20 kV. Sample 14 shows that with a quality edge fill, a 400-micron spacing could withstand up to 17 kV, which proves that even smaller edge margins could be used for capacitors designed for lower voltages.

Table 3. D3 Test Structure Testing Results

Sample ID	Dielectric Material	Measured Gap Spacing (mm)	Breakdown Voltage (kV)	Dielectric Strength (kV/mm)
2	Polystyrene	1.189	+20	16.821
4	Polystyrene	1.722	+20	11.614
10	Polystyrene	3.418	+20	5.851
11	Polystyrene	4.114	+20	4.861
12	Polystyrene	4.695	+20	4.260
13	Polyester	1.534	+20	13.038
14	Polyester	0.400	17.82	44.550
15	Polyester	1.819	+20	10.995
18	Polyester	1.580	19.57	12.386
19	Polyester	1.662	+20	12.034

After confirming that dielectric filled gaps could withstand high voltages, further experimentation needed to be done to determine if edge arc-over resistance of fully functioning capacitors could be improved. This was performed by winding capacitors with minimal edge margins and filling them with dielectric materials. The dielectrics chosen were ethylene acrylic acid (EAA) dissolved in xylenes and UVIKOTE® 7503 UV-curing urethane conformal coating. The capacitors were wound on a split mandrel. They contained approximately 100 tightly wound layers with approximately 20 linear feet of edge margin with a width of 0.1 in. on each side. Once each capacitor was wound, it was taped with Kapton to ensure it did not unravel when the mandrel was removed. The capacitor was then flattened during annealing.





*Figure 13. Capacitor Windings After Being Pressed and Annealed*

In this state, the edge margins can be filled using dielectrics and a vacuum desiccator. The capacitor was taped along its edge with Kapton tape to create a dam on one end. The test leads were also covered with tape to ensure they were not coated in dielectric. The dam ensured the fluid stayed on top of the windings until the vacuum was pulled, leaving the only way for the dielectric to travel was down the edge margins.



*Figure 14. Capacitors with Outside Dam Being Readied for Dielectric to be Placed Inside the Dam*

Four capacitors were built that were made with 1.2 mil thick Mylar and a 0.1-inch (2.54 mm) edge margin. Two of the capacitors were filled with EAA and two were filled with Uvikote. The capacitors were placed in a vacuum desiccator and vacuum was pulled down to 14 Tor for five minutes. The capacitors were then placed in a vacuum oven to cure the dielectric and pull any remaining air out of the windings. After processing in the oven, the capacitors were flipped, and the process repeated to the other end. This method worked well to get the dielectric between the windings but unfortunately coated the center of the capacitor, which was undesirable.

Four more capacitors were supplied but with 1.6 mil thick Mylar and 0.1-inch edge margin. This time a wider strip of Mylar was placed in the center near the mandrel to create

a dam to keep the dielectric from seeping into the center of the capacitor. The same process was used with taping to create the outer dam. In previous tests, the capacitors were able to tip or lean to one side leaving an accumulation of dielectric on either side but now the capacitors were held vertical inside the vacuum desiccator on a block of aluminum to mitigate tipping or leaning.

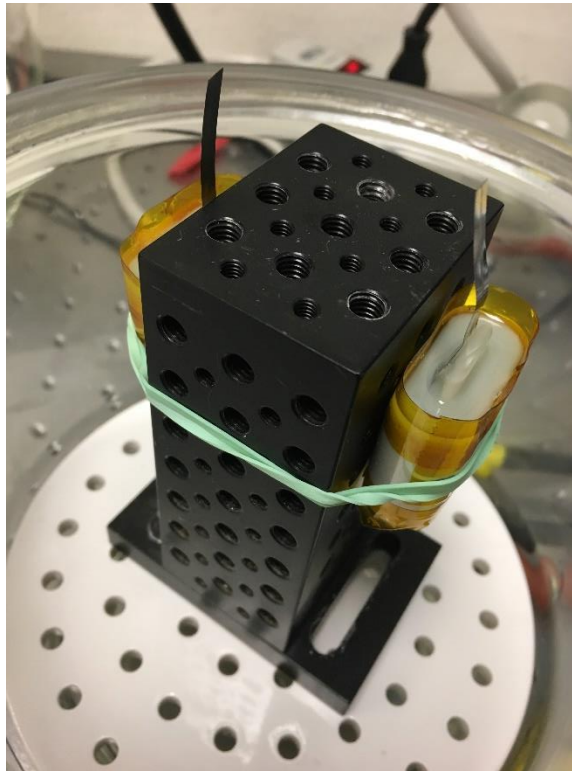


*Figure 15. Capacitors with Inside and Outside Dam Filled with Dielectric Prepped for Vacuum Process*

The 1.2 mil thick Mylar capacitors were tested to 4500 V and the 1.6 mil thick Mylar capacitors were tested to 6000 V. All eight capacitors were tested to failure and resulted in a 7% decrease in capacitance overall when compared to unfilled edge margin capacitors. The failure mode for these capacitors was from punch throughs. Punch through occurs

when the voltage pierces through the layers of Mylar. Some arcing was observed but was focused where the leads for the test probes were connected.

*Table 4. Results from withstand voltage screening*

<b>S/N</b>	<b>Mylar thickness (mils)</b>	<b>Fill material</b>	<b>Capacitance, pre-fill (nF)</b>	<b>Capacitance, post-fill (nF)</b>	<b>Leakage Current @ 3000 V/mil</b>	<b>Withstand voltage screen</b>
1-005	1.2	EAA	214	201	12.4	4500
1-006	1.2	Uvikote	216	213	46.1	4500
1-007	1.2	Uvikote	213	210	43.9	4500
1-008	1.2	EAA	207	197	20.4	4500
2-001	1.6	EAA		130	18.2	6000
2-002	1.6	Uvikote		105	47	6000
2-003	1.6	Uvikote		102	41	6000
2-004	1.6	EAA		107	16	6000

### 3.3 Reel-to-Reel

Traditional production of capacitors utilizes a Roll-to-roll or Reel-to-Reel (R2R) machine. This was used to make the precursor material for the capacitors. The machine is a Yasuei Seiki Minilabo™. This equipment was purchased with a Microgravure™ roller and extended laminator roller. This additional functionality offered the ability to combine two materials onto one roller rather than coating and rewinding one roll of material. This machine alone did not allow for enough material to be added at one time, so a second machine was constructed to be used in line with the Minilabo™, which expanded the capacity to include three more rolls of material.

The Microgravure™ technology allows for the gravure roller to be significantly smaller than the size of a standard gravure roller. This reduces the contact area between the substrate and the roller and allows for a larger web-to-roller distance. The larger web-to-roller distance allows for cleaner lines and less streaking (Assets: Mirwec Film).

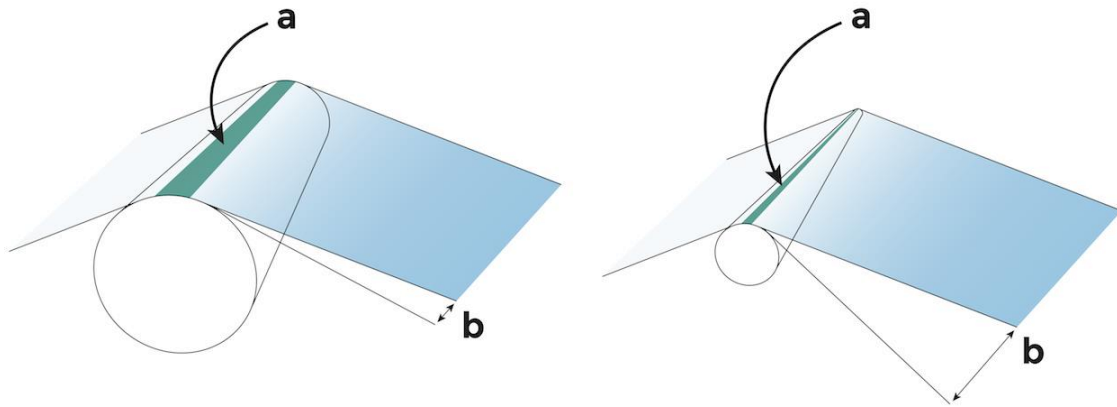


*Figure 16. Gravure to Microgravure Comparison of Contact Angle and Web-to-Roll Distance*

Gravure printing functions by having a roller rotating while partially submerged in the coating material. Excess material is then doctor bladed off before the web/film material meets the roller, as seen in Figure 17. Microgravure rods are engraved with a cross pattern which can be ordered to fit the viscosity of the coating material. For low viscosity materials (<200 cP), an 85R Microgravure rod can be chosen which was advertised to give a wet film of 13-22  $\mu\text{m}$ . Other mesh sizes were explored, including the 150R and 250R. The 150R and 250R mesh are advertised as coating a 4-9  $\mu\text{m}$  and 1-2  $\mu\text{m}$  wet film, respectively, but function with lower viscosity materials.

The film moves across the roller in the opposite direction as the roller is rotating, resulting in the material being transferred to the film by capillary forces. To achieve consistent coating of the film, a ratio between the diameter of the Microgravure rod and drive roller of the R2R machine must be maintained. The ratio is 1:16 for a line speed of 1m/min, which means for every full rotation of the drive roller the Microgravure rod rotates 16 times. This can be adjusted to affect the film thickness of the deposited material. By

increasing the ratio to 1:24, thicker coatings can be obtained and by reducing the ratio to 1:8 a thinner coating can be obtained (Chowdhury).

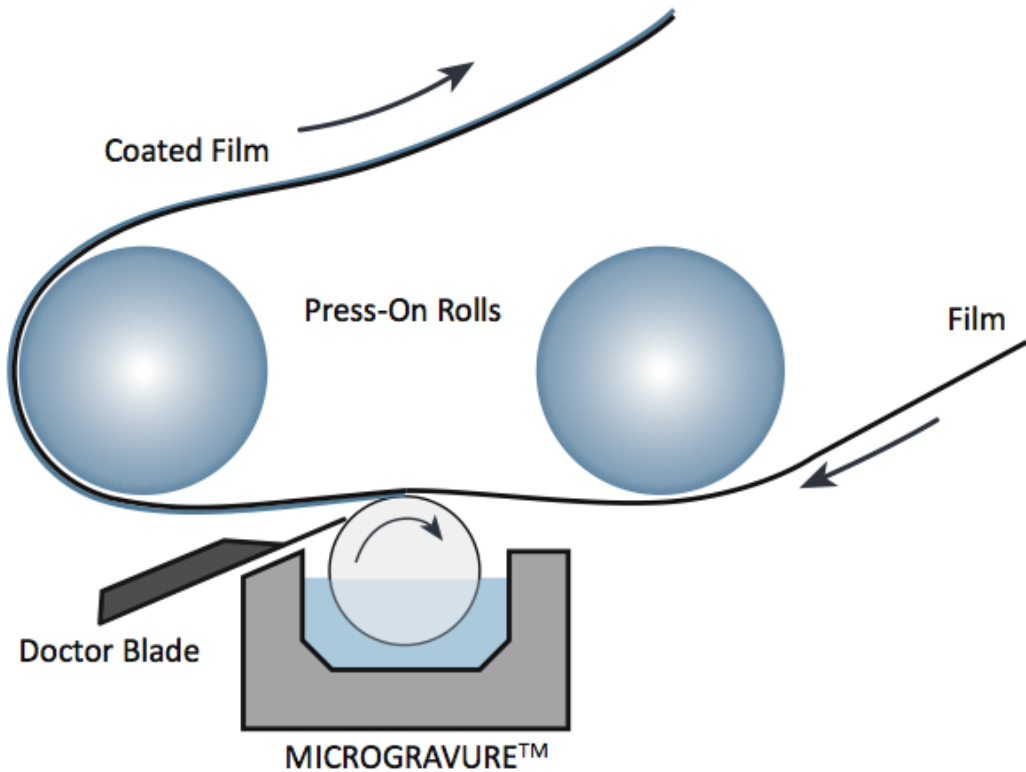


Figure 17. Diagram of the Microgravure Coating Process

Although the materials initially selected demonstrated great potential, they were solvent based, creating the possibility of trapping solvent between the Mylar layers. This necessitated the search for new materials. Acrylates are polymers that have yet to be crosslinked and are usually thermally or UV cured. Acrylates offer flexibility but often are solvent based. However, they remain thermally malleable after crosslinking so if the

solvent could be evaporated before applying a top layer of Mylar an acrylate could be used as edge-margin filler. One acrylate tested was Ethylene Acrylic Acid (EAA). EAA met the criteria of inexpensive, thermally or UV curable, and potentially adherable to PET or Mylar. The EAA came in pellet form and needed a solvent for dispersion. The EAA was mixed with Xylenes into different weight percentages varying from 8-25%.

*Table 5. EAA Dilution Measurements*

<b><i>Desired Weight Percent</i></b>	<b><i>Grams of EAA</i></b>	<b><i>Grams of Xylene</i></b>
8	30	322.5
15	30	172.00086
20	30	129
25	30	103.2

It was determined by rheology measurements and experimental results that 8-15 weight percent was the most compatible with the Microgravure™ roller. Mylar has such low surface energy that finding a compatible adhesive is difficult. With surface energy comes wettability. Wettability is a way of describing how liquids contact the surface of a material. Some liquids, like Xylenes, are more capable of spreading along a surface as opposed to forming beads. Mixing the low surface energy of Mylar with a non-polar solvent like Xylenes, results in the xylenes spreading across the surface of the Mylar. This becomes important when coating small sections of the Mylar with a xylenes-based ink. Normally, when applying a coating with the R2R, a clean edge is achieved with little to no spreading of the material. When the EAA mixture contacts the Mylar substrate it begins to



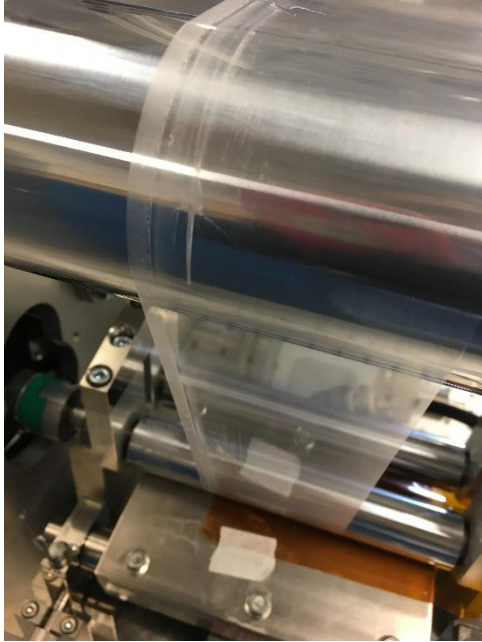


*Figure 199. EAA Coating Being Applied in a 5 mm Stripe Pattern on Left Edge of Mylar Demonstrating Smearing*

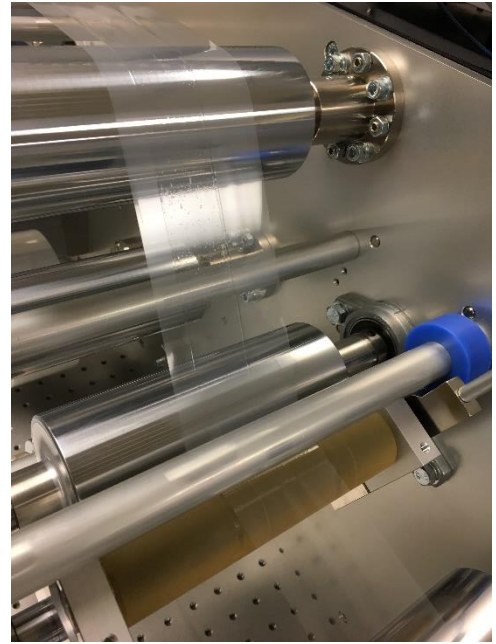


*Figure 188. Polystyrene Coating Being Applied in 25 mm Stripe Pattern at the Center of Mylar Demonstrating Clean Edges and no Smearing*

spread, leaving wavy edges and a smeared coating. This becomes an issue when attempting to mask the gravure roller to coat a 5 mm line onto the Mylar.

Another quality which becomes important is the pot life of the material. Pot life is the time the material can be worked with before it starts to set or cure. With solvent-based materials, some solvent may begin to evaporate causing the material to quickly change viscosity. Other thermally or UV curable polymers may start to crosslink while in the reservoir, causing the viscosity to increase or create agglomerations. The EAA material experienced both evaporation of solvents and agglomerates, resulting in inconsistent coating.

These inconsistencies directed the research toward a urethane. A urethane, often referred to as an epoxy, consists of one or two materials that are mixed and cured with humidity, temperature, UV, or the natural chemical reaction. One urethane considered was Uvikote™. Uvikote is a one- or two-part urethane that adheres to most plastics. It cures with all modes mentioned previously and has a low viscosity of <70 cP. Some negative aspects to Uvikote are its weak adhesion to Mylar and off gassing that has been reported by other users during curing.

Another urethane which has been approved for aerospace applications is Arathane 5753. Arathane is a 2-part urethane which cures by chemical reaction and can be sped up with increased humidity or temperature. Arathane passes the requirements for low to no off gassing and adheres well to most plastics. The pot life of Arathane is short but since it cures by reaction, the mixing of the material should be placed as close to the substrate as possible. One significant drawback to Arathane is that it becomes non-flexible after curing. Additionally, Arathane tends to wrinkle when wound around a ¼ inch mandrel. The wrinkles could cause defects in the coating leading to a breakdown points in the material.

A more systematic approach was needed to determine the limits of the coating system. Microgravure limited the viscosity to 200 cP, which meant more viscous and flexible materials like silicones could not be used. Looking into other coating methods like slot-die coaters or simple syringe dispensers would allow for higher viscosity materials and the mixing of components at the dispensing site. This has an additional benefit of having access to materials with a shorter pot life.

One approach was to have two syringe pumps work in tandem to extrude two-part silicones which would be combined via a mixing nozzle at the dispensing site. The syringe pumps would then create a continuous bead of adhesive over multiple hours. This process may lead to a build-up of excessive back pressure that could cause failure of the syringe pump, bursting of tubing, or syringe body. An analysis was completed considering the limitations on syringe pump force and speed, syringe force and volumetric flow rate, tubing diameter, and material viscosity. The volumetric rate of material is dependent on the width and thickness of the edge margin to be filled. It is important to note the greatest contribution to backpressure would be the smallest orifice the adhesive is to flow through. For this assessment, it was assumed that the tubing inside diameter was the smallest orifice and greatest contributor to backpressure.

To better illustrate the flow and calculations done in this experiment an example material is considered. Vitralit-UD 5134 is an acrylate material which adheres well to PET and other low surface energy substrates. It cures with ultraviolet or strong visible light. With a quick curing time and relatively low viscosity, it appears best suited for fast transfer rates and shorter reel-to-reel production times. Equation 4 can be used to calculate the Reynolds number. Flow tends to be more laminar at low Reynolds numbers and more turbulent at high Reynolds numbers. With laminar flow, the flow rate remains constant throughout the tubing, neglecting losses from friction associated with the tube walls.

In the equation,  $\rho$  is density,  $v$  is average velocity,  $L$  is length of tubing, and  $\mu$  is dynamic viscosity.

$$R = \rho v L / \mu \quad (4)$$

For Vitralit-UD 5134, the manufacturer's technical documents provide the following material properties:

*Table 6. List of Material Properties Used for Vitralit-UD 5134 Calculations*

<b>Density</b>	<b>12.7 kg/m<sup>2</sup></b>
<b>Dynamic Viscosity</b>	<b>25 Pa*s</b>
<b>Length of tubing</b>	<b>0.610 m</b>

Making practical assumptions about syringe pump placement, two extremes for tubing diameter are considered:

- Average velocity equals flow rate at syringe/cross sectional area of tubing range considered  
 Smallest diameter tubing =  $8.81\text{E-}10 / 3.16692\text{E-}9 = 0.278 \text{ m/s}$   
 Largest diameter tubing =  $8.81\text{E-}10 / 8.10731\text{E-}7 = 0.00109 \text{ m/s}$

The following Reynolds numbers were calculated for the smallest and largest tubing diameters considered.

$$R = \frac{12.7 * 0.278 * 0.6096}{25} = 0.08609$$

$$R = \frac{12.7 * 0.00109 * 0.6096}{25} = 0.3.3755E - 4$$

Using the Hagen-Poiseuille equation for viscous flow, a profile can be generated for the change in pressure from the syringe outlet to the tube outlet over a range of viscosities. Values are constrained to the limitations of the syringe pump. The tubing outlet is used rather than any spreading nozzle because the large spreading nozzle will provide no meaningful contribution.

The Hagen-Poiseuille equation uses dynamic viscosity  $\mu$ , pipe or tubing length  $L$ , volumetric flow rate  $Q$ , and cross-sectional area of pipe/tubing  $A$ .

$$\Delta P = \frac{8\pi\mu LQ}{A^2} \quad (5)$$

For the syringe pump's minimum and maximum dispensing forces, changes in pressure were calculated for commercially available tubing within a range of diameters. Results are shown in Figure 2020 and Figure 211. Pressure limits for the two available syringe bodies are also shown.

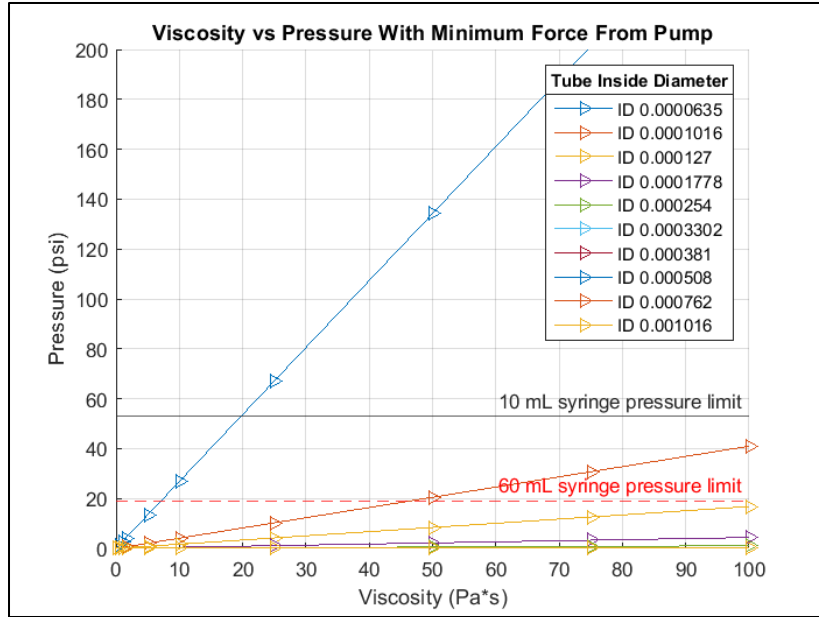


Figure 20. Viscosity vs Pressure with Minimum Force from Pump Over Various Tube Diameters to Narrow Options for Tube Purchase

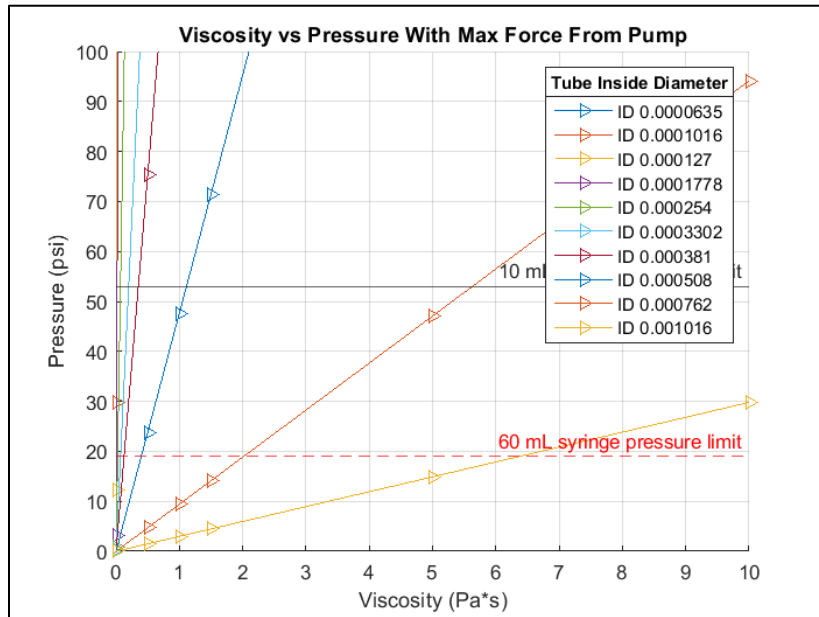


Figure 21. Viscosity vs Pressure with Maximum Force from Pump Over Various Tube Diameters to Narrow Options for Tube Purchase

From the calculations and other practical assumptions, suitable tubing can be selected. In the test scenario, a practical tubing length of 0.61 meters (24”) is selected with ID/OD of 0.0010/0.0016 meters (0.040/0.063 inches). It is important to note that the shorter the length of tubing, the smaller the change in pressure since backpressure is proportional to the length of tubing. Changes in pressure for varying flow rates are shown in Figure 2222 for a wide range of material viscosities. A comfortable safety margin to the pressure limit of the syringe must be established to ensure no over pressurization of the system.

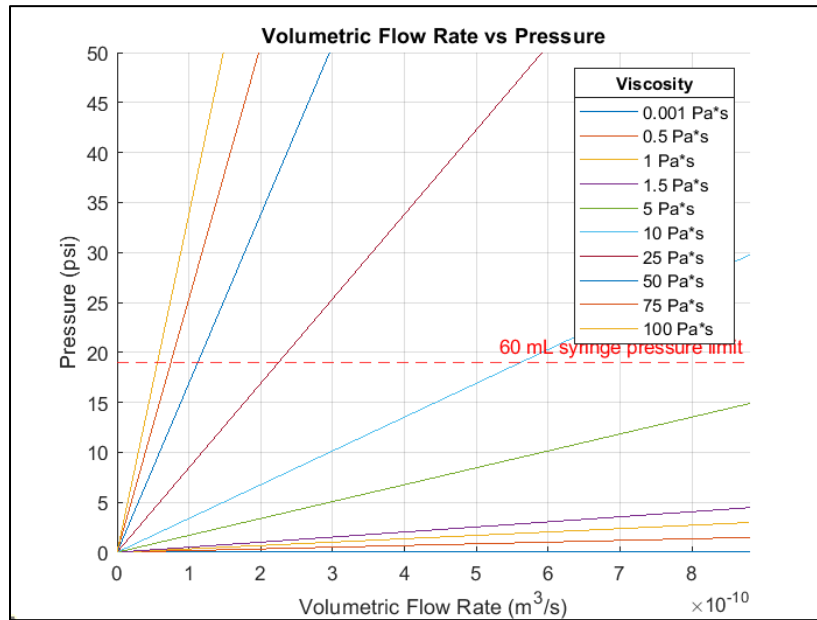


Figure 22. Volumetric Flow Rate vs Pressure to Determine Best Flow Rate for Variety of Viscosities

Figure 23 shows how pressure increases with fluid viscosity for a series of flow rates through the tubing selected above. The viscosity of various potential adhesives is shown as horizontal lines with the pressure limit of a 60 mL syringe body as the vertical

line. Following the data from Figure 22 volumetric flow rates for materials with certain viscosities can be determined, which assists in determining the back pressure that will be generated in the syringe pump system.

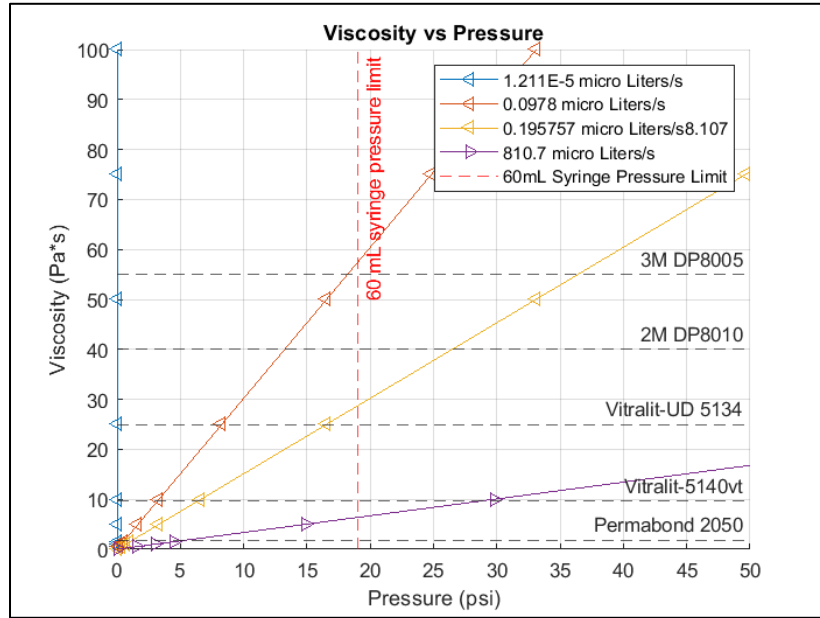


Figure 23. Viscosity vs Pressure with Potential Materials and Flow Rates

The viscosities associated with the materials in Figure 23 are listed in Table 7. These materials were selected from the list of potential materials as examples for a range of viscosities.



Table 7. Material Viscosity for Various Materials Considered in Figure 4

<b>Material</b>	<b>Viscosity (Pa*s)</b>
Permabond 2050	1.8
Vitralit-5140vt	9.6
Vitralit-UD 5134	25
3M DP8010	40
3M DP8005	55

The information from Figures 22 and 23 were used to generate a table of maximum flow rates for each viscosity and the time it would take to produce a roll of pre-cursor material.

Table 8. Table of Maximum Flow Rates and Machine Speed for Range of Viscosities

<b>Viscosity (cP)</b>	<b>Volumetric flow rate (m<sup>3</sup>/s)</b>	<b>Transfer Rate (m/h)</b>	<b>Time to produce one roll (hours)</b>	<b>Machine Speed Required (m/min)</b>	<b>Machine Speed Required (ft/min)</b>
1	8.81E-10	634.32	2.07	10.57	34.69
500	8.81E-10	634.32	2.07	10.57	34.69
1000	7.83112E-10	563.84	2.32	9.40	30.83
1500	7.83112E-10	563.84	2.32	9.40	30.83
5000	7.83112E-10	563.84	2.32	9.40	30.83
10000	5.87337E-10	422.88	3.10	7.05	23.12
25000	1.95787E-10	140.97	9.30	2.35	7.71
50000	9.78996E-11	70.49	18.59	1.17	3.85
75000	1.21167E-14	0.0087	150233.42	0.00015	0.0005
100000	1.21167E-14	0.0087	150233.42	0.00015	0.0005

## Chapter 4

## 4.1 Conclusion

The data collected and the initial experiments performed in this research demonstrate that filling the edge margins will increase the reliability and decrease the size of high voltage Mylar capacitors. Initial tests with solvent based materials demonstrated that a gap spacing of less than 1 mm could withstand near 20 kV. Tests with Urethanes also demonstrated that gaps of less than 1 mm could withstand near 20 kV. The experiments performed on impregnated capacitors demonstrated a decrease in capacitance which was not expected. Selecting a material is a crucial step that dictates the coating method. Materials such as urethanes or silicones that are not solvent based remain the focus of this project. Unfortunately, time was limited, and no tests of the newly designed syringe pump coating method were performed. However, this research's initial finding that within the specified viscosity range, the syringe pump system will work to apply a bead of material along the edge of the Mylar to create the pre-cursor material. With the research conducted it can be concluded that filled-edge margins with the extended-foil design will decrease the size of the edge margin and effectively increase the reliability of high voltage capacitors by creating a barrier to keep out FOD and VOCs.

## 4.2 Future Work

In continuation of previous experimentation and data collection, materials will be tested in the same fashion as prior experiments. Research continues in the effect to identify and test materials from multiple suppliers, including Dow, MasterBond, and Silicone Solutions. In conjunction with this project, producing a custom R2R extension which will increase the number of rolls the Mirwec system can manage at one time needs to be completed before capacitors can be produced. This custom R2R is crucial in supplying the alternating layers of foil and Mylar required to form the capacitors. Once a material is selected that meets the needs of the customer, the process of coating and forming the precursor material can take place. With several rolls of pre-cursor material made, capacitors can be seamlessly formed using the Mirwec and custom R2R system. After production of the new capacitors, thorough testing will be conducted to ensure reliability and function.

During the production of capacitors many considerations need to be made on the effects of curl, thermal expansion, strain mismatch, and shrinkage associated with the lamination process. Strain mismatch can affect the winding process due to the foil and PET materials being wound together. The foil is not as ductile as the Mylar which has a high modulus of elasticity. During the winding and lamination process consideration needs to be taken to address these issues and perhaps some modeling can be done to better understand the differences between machine direction curl (MD) and transverse direction curl (TD) along with predictions for thermal expansion during storage. There are many papers out that discuss the modeling of webs using lamination theory. One such paper uses

Abaqus to develop a process for modeling viscoelastic materials to determine the amount of creep and curl that will affect rolls of material that are stored in unmodulated environments. (Pan)

There are large companies that have had success with roll-to-roll processes who often release content to further the knowledge of film behavior and the effects of biaxial stresses in PET films. One such paper from 3M was released in 2009 that discusses how to overcome curl and inverse-curl when bringing multiple webs together under nip rollers. (Kidane) These papers along with many others will help direct the process of producing capacitor pre-cursor material and eventually capacitors.

## Works Cited

- "Assets: Mirwec Film." n.d. *Mirwec Film Incorporated Web Site*. Brochure. 28 December 2019.
- Brooks, R.A. & Edwards, L.R. "A close-tap pair design of buried-foil capacitors." 1 February 1996.  
*University of North Texas Digital Library*. Web Document. 24 February 2020.
- Chowdhury, R.A., Clarkson, C. & Youngblood, J. "Continuous roll-to-roll fabrication of transparent cellulose nanocrystal (CNC) coatings with controlled anisotropy." *Springer Nature* 05 February 2018: 1769-1781.
- Deken, B., Pekarek, S. Dogan, F. "Minimization of field enhancement in multilayer capacitors."  
*Computational Materials Science* (2006): 401-409. Journal.
- Herzberger, Jaemi Lee, and Tanner, Danelle Mary. "Failure Mechanisms in High Voltage Mylar Capacitors." 1 January 2014. *Office of Scientific and Technical Information*. Document. 25 February 2020.
- Jr., John M. Santiago. *Circuit Analysis for Dummies*. Hoboken: John Wiley & Sons, 2013. 193-196. Book.
- Kidane, Sam. "Laminate Theory Based 2D Curl Model." (2009).
- Pan, Sheng. "The Mechanics of Winding Laminate Webs and the Prediction of Machine Direction Curl."  
PhD Dissertation. 2019.
- Sharma, Ravindra Kumar. "Development of Compact High Voltage Low Inductance Energy Storage Pulse Capacitors." *Barc Newsletter* 2015: 175-178.
- Sorbent Systems. *What is Mylar*. 2016. Website. 18 November 2018.
- Wooley, M.C., Kohman, G.T., McMahon, W. "Polyethylen Terephthalate - Its Use as a Capacitor Dielectric." *Transactions of the American Institute of Electrical Engineers* (1953): 33-37. Journal.

## Appendix

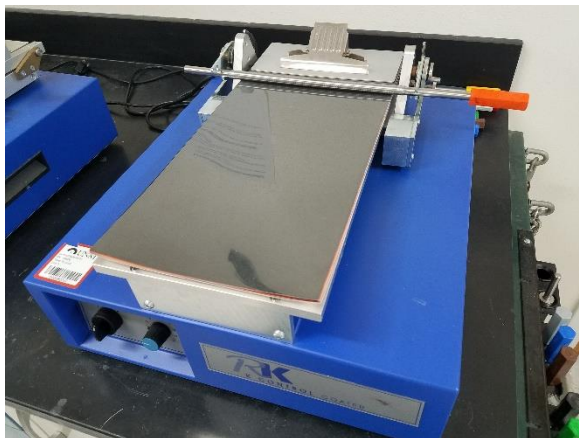


*Figure 24. RK Meyer Rod Coater Used in Initial Experiments*



*Figure 25. Aluminum block with Foam Used After Determining Film Thickness was Independent of Speed and Pressure*